Industrial Engineering Journal
ISSN: 0970-2555
Volume : 53, Issue 5, May : 2024

"SYNTHESISANDCHARACTERIZATIONOFBIODEGRADABLEPOLYMERNANOCOMPOSITESFORPACKAGINGAND BIOMEDICAL APPLICATIONS"

KRANTI DHRUW [1]SURAJ KUMAR JAISWAL[2] AMIT KUMAR MOHIT[3]KARUNANIDHI BHAGAT[4] DEVENDRA KUMAR[5]

[1]Government Engineering College, Raipur, Sejbahar, Old Dhamtari Road, Chhattisgarh, PIN-492015

Keywords:Biodegradable,biomedical,naturalpolymers,Nanocomposites, packaging.

ABSTRACT:

Endlessly renewable natural resources, such as plants, animals, and microorganisms, offer a sustainable source for extracting natural polymers. These materials decompose easily into simple compounds like water, carbon dioxide, and inorganic molecules through the action of natural bacteria and enzymes, making them environmentally friendly and biodegradable. In this investigation, we focus on bio-degradable polymers derived from plant starch. By extracting starch molecules from plants and introducing a small amount of plasticizer along with other additives, we create thermoplastic starch resin. This type of plastic shows great promise as it can completely degrade in natural environments. The order in which components (starch, plasticizer, glycerol, clay) are added significantly influences the properties of the resulting composites. Additionally, nano metal oxide particles, sourced from various plant parts such as leaves, roots, stems, and seeds, are utilized to enhance the composites' properties. Following the completion of sample preparation, a series of tests and analyses are conducted, including Mechanical Testing (such as Tensile, Impact, and Tear tests), Thermal Analysis (including Melt Flow Index, Rheological Analysis, Thermal Conductivity, and Thermal Diffusivity), Morphology assessment (SEM, TEM), DSC & TGA tests, and Biodegradation Tests under various conditions (Controlled Industrial Composting Conditions, Controlled Composting Conditions at Ambient Temperature, Anaerobic Digestion, Soil Biodegradation Test, Marine Biodegradation, Biodegradation in Aerobic and Aquatic Conditions, and Aqueous Anaerobic Biodegradation Test).In the context of this research, it is anticipated that improvements will be observed in the mechanical strength of the polymers, as well as enhancements in physical and optical properties, antibacterial features, and microbial activities of the composites. Consequently, these resulting composites can be effectively utilized in packaging and biomedical applications. They offer a viable alternative to certain non-biodegradable plastics, reducing the burden on landfills and open dumps by being redirected towards compost, anaerobic digesters, or soil systems.

INTRODUCTION :

Backgroundofthestudy

Composite materials, characterized by the combination of two or more distinct components to achieve desired enhanced qualities, have a rich history dating back to ancient civilizations. Around 1500 B.C., Mesopotamians and Egyptians ingeniously utilized mud to bind straws together, constructing shelters. Following this, the Mongols demonstrated the use of composites by crafting bows for hunting, using natural pine as a binding material reinforced with bone, wood, or horns, resulting in bows that were formidable weapons until the advent of firearms.The late 1800s marked a significant turning point with the emergence of synthetic resins through polymerization processes, ushering in what is often referred to as the "plastic era." Bakelite, melamine, and celluloid were

among the earliest synthetic resins developed during this period. The proliferation of plastics such as polyester, vinyl, styrene, and phenol resins followed suit. Concurrently, innovations like glass fiber, pioneered by Owens Corning, revolutionized polymer composites, offering enhanced reinforcement and durability. World War II saw the rise of lightweight novel composites, with fiber-reinforced composites emerging as viable alternatives in military applications. Post-war, fiber-reinforced composites gained popularity, notably with Brandt Goldsworthy's development of the glass fiber surfboat and the pultrusion process for fabricating glass fiber-reinforced composites. Goldsworthy is widely recognized as the "Grandfather of Composites" for his significant contributions to the field.
In the late 1960s, the introduction of carbon and aramid (kevlar) fibers marked another milestone in composite materials. Carbon fiber-reinforced composites found applications as substitutes for steel, offering exceptional strength-to-weight ratios. Meanwhile, aramid composites proved ideal for body armor due to their high impact resistance. Today, the composite industry continues to evolve, leveraging the exceptional ability to effectively combine materials to deliver superior properties across a diverse range of applications.

CURRENTSTATUS :

Plastics have become an integral part of our daily lives due to their numerous beneficial qualities. Their low density, strength, durability, versatility in design and production, and cost-effectiveness have driven their widespread adoption. These characteristics have led to their utilization in various sectors, including industrial and automotive applications, as well as packaging materials. With their diverse uses, such as in food preservation and distribution, it is unsurprising to find a significant portion of Plastic Solid Waste (PSW) in the overall stream of Municipal Solid Waste (MSW). As global population growth continues and consumer habits foster a throw-away culture, there is a steady increase in the generation of municipal solid waste from residential, commercial, and institutional sources. However, landfills have finite capacities and can only accommodate a limited amount of waste before they begin to pose environmental hazards, contaminating soil, water, and air. This underscores the pressing need for sustainable waste management practices to mitigate the adverse impacts of plastic waste on

PROBLEMS ASSOCIATED WITH CONVENTIONAL PLASTICS

Since the widespread industrial use of synthetic polymers began in the 1940s, plastic products have transformed various industries, significantly impacting material research. While plastics offer numerous advantages such as excellent corrosion resistance, processing flexibility, and low manufacturing costs, they also pose significant environmental challenges throughout their lifecycle.

1. The manufacturing process of plastic products contributes to greenhouse gas emissions, exacerbating climate change. Additionally, the properties that make plastics valuable also make their waste management challenging. Currently, only a small fraction of plastic waste is recycled due to contamination and technical limitations.

2. Furthermore, plastic waste accumulates in the environment, particularly in oceans where vast garbage patches, comprising around 80 percent plastic, have formed. Plastic debris can persist in ecosystems for centuries, particularly in marine environments, posing threats to wildlife.

3. In many developing nations, the predominant method of municipal waste disposal involves dumping plastic waste in public spaces due to inadequate waste management infrastructure and public resistance to establishing new disposal sites. Implementing strategies like waste minimization and recycling is crucial to prolong the lifespan of existing disposal sites and mitigate environmental impacts.

4. Plastic waste pollution is a growing concern, as plastics can act as carriers of water-soluble pollutants, posing risks to aquatic life. Despite the rising costs and poor biodegradability of

petroleum-based plastics, conventional landfilling remains prevalent, while alternatives like incineration raise concerns about air pollution and hazardous ash production.

5. Globally, inadequate waste management procedures contribute to the persistence of plastic waste, leading to environmental degradation on land and in oceans. Improper disposal methods, such as open burning, not only pose health risks but also contaminate waterways and oceans, further exacerbating the plastic pollution problem.

6.Plastic waste accumulation in oceans, comprising both microplastics and larger debris, is a global issue driven by ocean currents rather than the origin of the waste. This accumulation harms marine life and facilitates the transfer of contaminants and organisms, perpetuating environmental degradation. Addressing these challenges requires concerted efforts to improve waste management practices, promote recycling, and develop sustainable alternatives to conventional plastics.

Descriptionoftheexperiment
procedureofexperiment
The methodology of the proposed research workconsistsofthe followingsteps:
Synthesisofbiodegradablepolymerandthenanoparticles: The biodegradable Nano composites will bepreparedfromtheplant-basedmonomers using polycondensation/ ringopeningpolymerization.

I. The metal/ metal oxide nanoparticles willbe prepared using the plant extracts suchasleaves,stems,rootsetc.

2. SynthesisofbiodegradablepolymerNanocomposites:

I. ThebiodegradablepolymerNanocompositessampleswillbepreparedbased on the design of experiments as perthefullfactorialdesignmodelL-27.Therefore, a total of 27 compositions willbe preparedforeachofthe outputs.
II. 3sampleswillbepreparedforeachcomposition.

The production of PLA (polylactic acid) involves several distinct stages, each contributing to the overall process:

1. **Sugarcane Cultivation**: Sugarcane is grown in various provinces, covering approximately 8% of the total arable agricultural land. The cultivation process includes land preparation, planting, maintenance, and harvesting stages. Fertilizers, including both chemical and biofertilizers, are commonly used. Some farms utilize filter cake from sugar mills as a soil conditioner. Harvesting is typically manual, with some farmers resorting to pre-harvest burning to facilitate easier manual harvesting. However, efforts are being made to reduce burning due to its negative environmental impacts.

2. **Sugar Mill Processing**: At the sugar mill, cane is crushed to extract juice. Bagasse, the fibrous residue remaining after crushing, is burned to produce electricity and heat. The cane juice undergoes clarification using heat and chemicals to remove impurities, followed by evaporation, crystallization, and centrifugation to produce raw sugar and molasses. The filter cake from clarification is commonly used as a soil conditioner.

3. **Lactic Acid Production**: Corbion produces lactic acid through the fermentation of cane sugar. Lime is added to control pH, leading to the formation of calcium lactate. Nutrients are

introduced to aid fermentation. The resulting fermentation broth is concentrated, and calcium lactate is acidulated with sulfuric acid to recover crude lactic acid. This process generates gypsum as a by-product, which is removed by filtration. The lactic acid undergoes purification to remove impurities, yielding lactic acid and stillage as by-products, with various applications such as animal feed and biogas production.

4. **Lactide and PLA Production**: Total Corbion PLA produces lactide through the polymerization of lactic acid. After polymerization, any remaining lactide monomer is recycled within the PLA production process. The polymer undergoes further purification to produce PLA pellets, which serve as the final product.

Overall, the production of PLA from sugarcane involves a series of interconnected processes, utilizing various inputs and generating valuable by-products. Efforts are being made to optimize efficiency, reduce environmental impact, and maximize resource utilizationthroughout the production chain.

Industrial Engineering Journal
ISSN: 0970-2555
Volume : 53, Issue 5, May : 2024

(ii)Synthesisofbiodegradablenanoparticles

SynthesisofNeem(Azadirachtaind ica)seedextract

Fresh Azadirachta indica seeds are harvested, cleaned, and air-dried in shade to remove any moisture. Once dried, they are finely ground into a powder. Approximately 10 grams of this powder is then added to a round-bottom flask and mixed with a solution of methanol and water in a 9:1 ratio. The mixture undergoes continuous magnetic stirring on a hot plate maintained at a temperature of 95°C, with a stirring speed of 350 rotations per minute. This stirring and heating process is carried out for 3 to 4 hours to ensure efficient extraction of phytoconstituents from the seeds.After extraction, the mixture is filtered using Whatman filter paper No. 42 to separate the solid residue from the liquid extract. The filtrate obtained after filtration contains the desired seed extract, which is rich in various phytoconstituents. This seed extract acts as a stabilizing agent for the synthesis of zinc oxide (ZnO) and magnesium zinc oxide (MgZnO), enhancing the stability and properties of the synthesized materials.

SynthesisofMg@ZnOandZnOnanoparticles

In the synthesis process of ZnO nanoparticles, a 4-gram precursor of zinc acetate dihydrate is placed into a round-bottom flask and mixed with 10 ml of deionized water. The mixture is stirred continuously on a magnetic hot plate at a temperature of 75°C until a homogeneous solution is achieved. Then, the seed extract is added dropwise to the precursor solution in a separating funnel while maintaining magnetic stirring at 450 rotations per minute overnight at a low temperature of 10°C. Subsequently, centrifugation is carried out at 900 rotations per minute for 15 minutes, and the resulting filtrate is dried at 65°C. This is followed by calcination at 500°C for 2 hours, leading to the biosynthesis of ZnO nanoparticles. For the synthesis of Mg@ZnO nanoparticles, in addition to the precursor salt, 5 grams of dopant magnesium tetrahydrate is mixed with 10 ml of deionized water in a round-bottom flask and heated on a hot plate with continuous stirring at 75°C. The plant seed extract is slowly added to the precursor solution in a separating funnel. Subsequently, sonication is carried out for 10 minutes, followed by centrifugation at 10,000 rpm for 15 minutes. The resulting product is dried in an oven and then subjected to calcination at 450°C, resulting in the formation of Mg@ZnO nanoparticles. Both the biosynthesized Mg ZnO and ZnO nanoparticles undergo further characterization using various analytical techniques to study their properties and morphology. This synthesis process represents an eco-friendly approach utilizing plant seed extract as a stabilizing agent for the production of nanoparticles, contributing to sustainable nanomaterial synthesis.

Synthesisofiron3phosphate

The synthesis process of navy particles using datura leaves extract is described as follows:
1. Aqueous extracts of datura leaves, with a concentration of 20.0 g L^-1, are prepared by heating the solution at 353 K for 1 hour. After cooling to temperatures between 298.15 K and 300.15 K, the extracts are filtered to remove any solid residues.
2. Separately, a solution of FeSO4.7H2O with a concentration of 0.1 M is prepared.
3. The datura leaf extract in powder form is then added dropwise into the Fe(II) solution at a 1:1 ratio, while maintaining a temperature of 298.15 K, under magnetic stirring for 30 minutes.
4. Subsequently, the Fe nanoparticles are washed multiple times with ethylene to remove any residual FeSO4. The iron colloids are then left to dry overnight, resulting in the synthesis of iron nanoparticles using the dry leaves of datura.
Before and after the adsorption of phosphorus, the synthesized iron nanoparticles (referred to as GFe-n and WFe-n) are characterized using various analytical techniques:

- X-ray diffraction (XRD) analysis is performed to study the composition of the nanoparticles.
- Fourier-transform infrared spectroscopy (FTIR) is utilized to analyze surface functional groups present on the nanoparticles.
- Scanning electron microscopy (SEM) is employed to examine the morphology of the nanoparticles.
- Transmission electron microscopy (TEM) is utilized to further investigate the size and morphology of the nanoparticles.
- Dynamic light scattering (DLS) analysis is conducted to determine the zeta potential of the samples.

These characterization techniques help to understand the composition, surface properties, morphology, size, and zeta potential of the synthesized iron nanoparticles, both before and after phosphorus adsorption. This synthesis method offers a sustainable approach utilizing natural plant extracts composite.

We employ a method to prepare our final samples involving PLA (polylactic acid) mixed with nanoparticles in chloroform. The process entails the following steps:

1. **Preparation of PLA and Nanoparticle Solution**: PLA and nanoparticles are mixed in chloroform, and the mixture undergoes continuous rotation in a magnetic stirrer until a homogeneous solution is achieved. This ensures uniform dispersion of nanoparticles within the PLA matrix.
2. **Vacuum Chamber Treatment**: After mixing, the solution is transferred to a petri dish and placed in a vacuum chamber for a duration of 12 to 14 hours. This step aims to remove any remaining chloroform solvent from the solution, leading to the formation of a solid film.
3. **Sample Preparation**: The solid film obtained from the vacuum chamber is then shaped into dog bone specimens. These specimens are standardized in size and shape, ensuring consistency across samples.
4. **Final Sample Preparation**: The prepared dog bone specimens, containing the PLA-nanoparticle composite, represent our final samples for analysis and testing.

The entire process is conducted with careful attention to detail to ensure the integrity and reproducibility of the final samples. The resulting specimens are ready for further characterization and evaluation, as depicted in the accompanying figure. This methodology underscores the importance of precise sample preparation techniques in research and development endeavors.

RESULT

Theresultoftheproposedresearchworkareasfollows:

(i) Themechanicalstrengthofthepolymersmaybeimproved.

(ii)

(iii) Thephysicalandopticalpropertiescompositesmaybeimproved.

(iv) Antibacterialpropertiesandmicrobialactivitiescomposites maybe improved.

(v) Thecompositescanbesuggestedforpackagingandbiomedicalapplication

Industrial Engineering Journal
ISSN: 0970-2555
Volume : 53, Issue 5, May : 2024

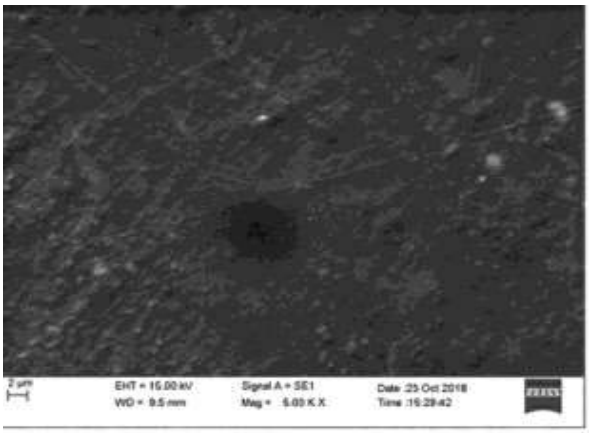

(a) 5% CaP

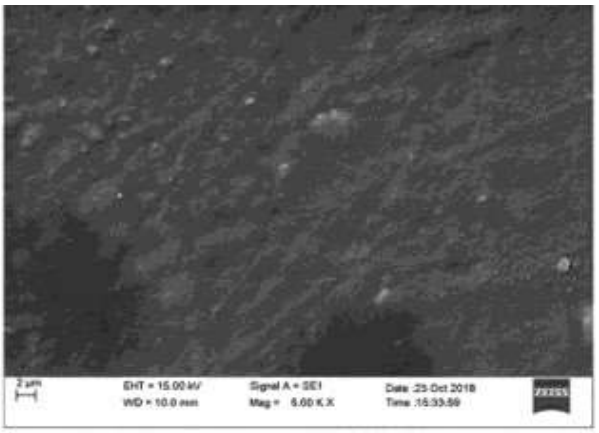

(b) 10% CaP

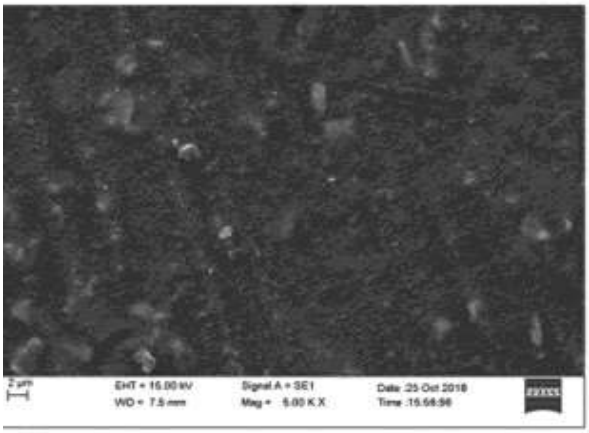

(c) 15% CaP

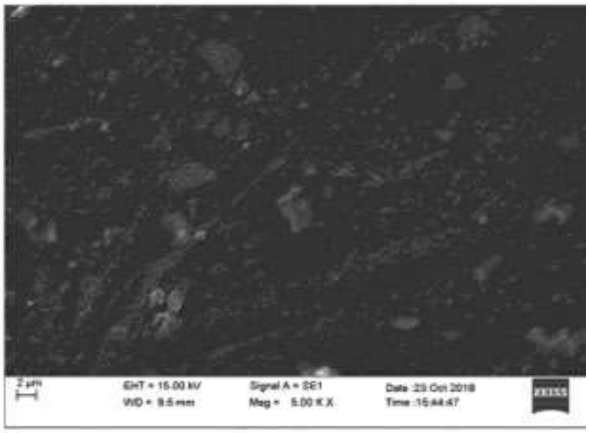

(d) 20% CaP

CHARACTERIZATIONS

The size and distribution of the CaP nanoparticles were analyzed using a Zetasizer (Nano ZS, Malvern Instruments). This instrument utilizes dynamic light scattering (DLS) to measure particle size and distribution in a solution.

Scanning electron microscopy (SEM) was employed to study the surface morphology of the nanocomposite film. Before SEM analysis, the sample underwent coating with a very thin layer **of gold to enhance conductivity and imaging quality.**

Tensile testing of the nanocomposite film was conducted at room temperature using a universal testing machine (INSTRON dark series 7200). The crosshead speed

SAMPLE

Industrial Engineering Journal
ISSN: 0970-2555
Volume : 53, Issue 5, May : 2024

was set to 5 mm/min during the tensile test. Five test samples were examined for each composition, and the average tensile strength values were plotted.

The melt rheology of the PLA nanocomposite films was evaluated using a rotational rheometer (MCR 102). This measurement was performed using a 25 mm diameter parallel plate geometry in the dynamic frequency sweep mode. The experiment was carried out in a nitrogen atmosphere at 180°C. The frequency test was conducted in the angular frequency range of 1-500 rad/sec, maintaining a constant strain within 5%.

These characterization techniques provide valuable insights into the properties and behavior of the nanocomposite films, aiding in their optimization for various applications. rate.

RESULTS AND DISCUSSION

MorphologyOf nanoparticles

Scanning electron micrographs displayed in Figure 2 depict razor-cut surfaces of silicone elastomer nanocomposites. These images reveal that a uniform dispersion of multi-walled carbon nanotubes (MWCNTs) was achieved within the silicone matrix, up to a loading of 4 wt%. Beyond this threshold, agglomeration occurs. Nevertheless, the interconnectivity among these agglomerates forms a continuous network within the rubber matrix, facilitating easy electron passage under external electric fields. The darker regions in the images represent the polymer matrix, while the brighter areas depict the MWCNTs. At lower MWCNT loadings, there is no distinct observation of a double-phase structure due to partial compatibility between the silicone elastomer and MWCNTs. The micrographs also demonstrate a uniform distribution of MWCNTs across all filler loadings, with a majority of individual nanotubes rather than aggregates, indicating complete exfoliation of the nanotubes within the silicone matrix. This dispersion can be explained in terms of colloids, where absorbed polymer stabilizes the nanotube dispersion, guarding against bridging flocculation and depletion aggregation induced by free polymer. Further analysis of the SEM micrographs reveals homogeneous dispersion of MWCNTs in the polymer matrix, with aggregation occurring as filler loading increases. This phenomenon is particularly evident in the micrographs of samples with 6% MWCNT loading. Maintaining a good distribution of MWCNTs within the silicone matrix is crucial, as agglomeration or sedimentation may lead to inferior material properties. Thus, achieving a remarkably uniform distribution of MWCNTs in the silicone matrix is essential for optimizing nanocomposite performance.

Industrial Engineering Journal
ISSN: 0970-2555
Volume : 53, Issue 5, May : 2024

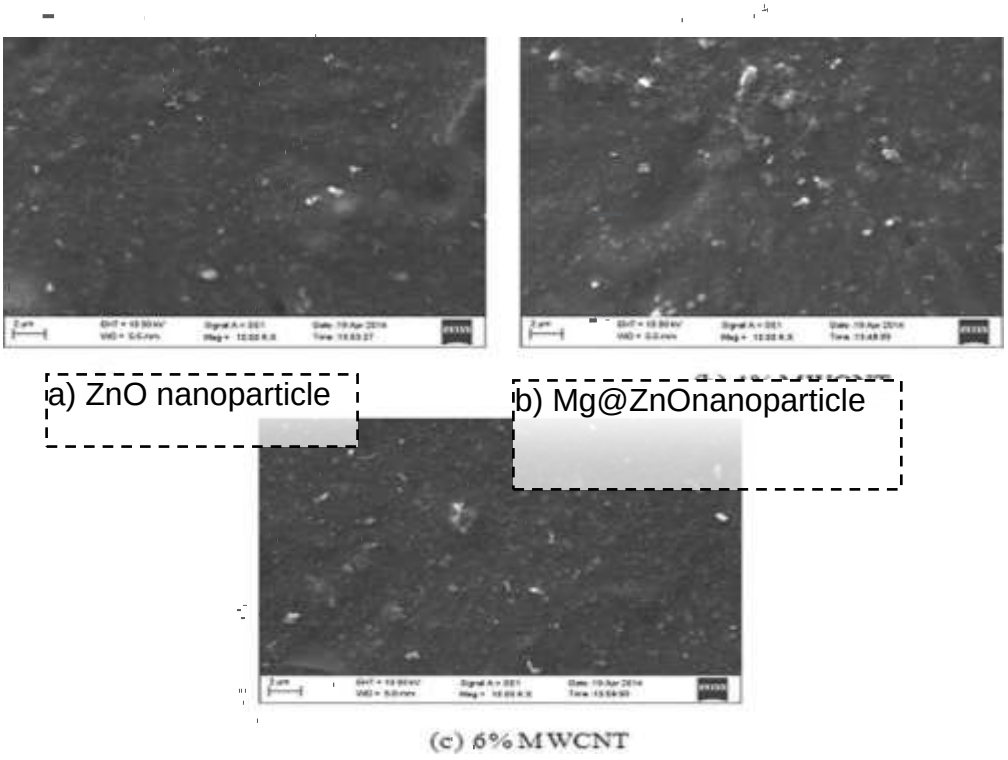

Figure2.(a)–(c)SEMphotomicrographsofMWCNT-filled nanoparticles(ZnO,Mg@ZnO,FePO4).SEM:scanningelectronmicroscopy;MWCNT:multiwalledcarbonnanotube.

observed. There are little or no observable voids betweenthe matrix and the MWCNTs, which confirms the goodcompatibilityofMWCNTswiththesiliconematrix.

Similarly, theho mogenousdi spersionofNPsinthepolymer matrix is important, because any inhomogeneitywouldeventually lead to structural defects in the compositestructure. To study the dispersion of NPs in the polymermatrix,amorphologicalinspectionisrequired.Themicrographs of SIR nanocomposites containing differentloadingsofNPsare shown in Figure 3. It is evident that NPs particles arerandomly oriented throughout the silicone matrix, and thusan interconnecting network is formed. In Figure 3(a), NPsparticles are dispersed individually in the silicone matrix.The zinc/NPs nanocomposites with 6% (Figure 3(c))and8%(Figure3(d))NPsloadingsalsodisplaygooddispersion,eventhoughsmallagglomeratesappear withanincrease in the NPs loading. The SEM micrographs alsoshow that the conductive network density is increased withanincreaseintheNPscontent.

HR-TEManalysis The reinforcing effect of nanofillers in a polymer matrixdependsontheirdegreeofdispersioninthepolymer matrix. Hence,morphological analysisis very importantfor the evaluation of filler dispersion in the polymer matrix.To study the dispersion of MWCNTs in the nanoparticle matrix,the morphology of the SIR/MWCNT nanocomposites wasinvestigated by HR-TEM and the micrographs of 2%, 4%,and6%MWCNT-loadedSIRnanocompositesarepresentedinFigure4(a)to(c).Figure4(a)and(b)showsanabundance of well-dispersed nanotubes throughout the Sirmatrix without any agglomerates. In Figure 4(c), it is seenthat the dispersion of MWCNTs is poor due to the presenceof some agglomerates. These agglomerates reduce the rein-forcing effects of MWCNTs, because they act as flaws inthe polymer matrix. This may lower the properties of thecomposite. However, the average diameter of the MWCNTinSIRmatrixisfoundtobe ≈ 20nm. ThedispersionofNPs intheSirmatrixwas

Industrial Engineering Journal
ISSN: 0970-2555
Volume : 53, Issue 5, May : 2024

also observed in the HR-TEM micrographs (Figure 5(a) to(d)). The dark spots in the micrographs were identified asNPs, and they show very good “exfoliation” within the Sirmatrix; in this context, exfoliation refers to how well theNP particles are de-aggregated. There are, however, someregions in which NPs shows a small degree of aggregation.This is to be expected, since these NPs were notmodifiedpriortoincorporationintheSIRmatrix.

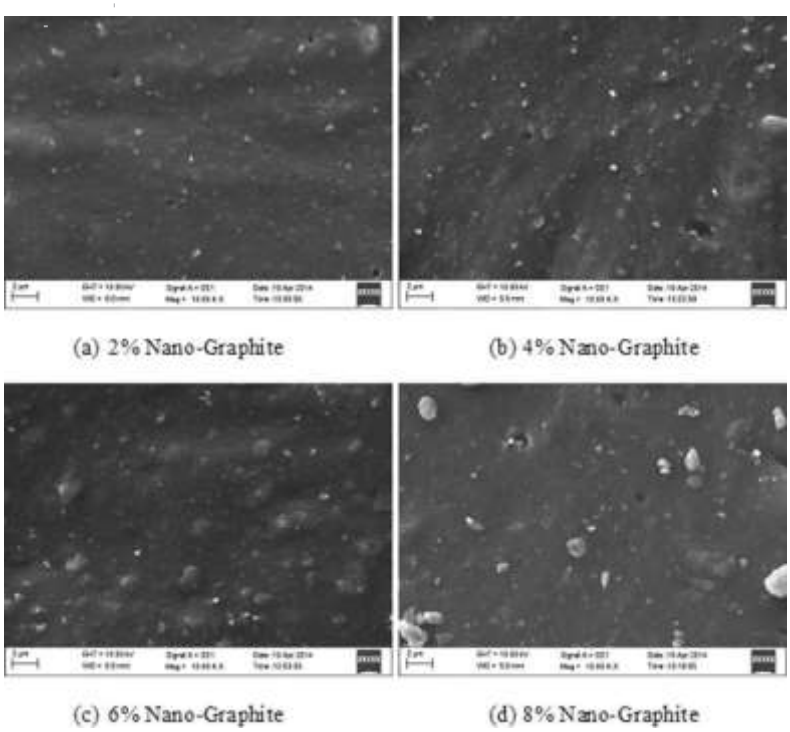

Figure3.(a)–(d)SEM nanoparticle(ZnO,Mg@ZnO,FePO4,Ag2O).SEM:scanningelectronmicroscopy.

The images also show anexcellent alignment of the matrixalong the fiber axis. The alignment of the polymer chainsalong with NPs leads to an enhancement in the compositematerial’smechanicalproperties.Anotherfactorconsidered importantforgoodmechanical properties isthe aspect ratio. If the aspect ratio is high, the strength ofthe materialwouldbe high.Inthecaseofthe6%and8% NPs-reinforced zinc,silver nanocomposites, agreaternumberoflargeragglomerateswereobserved.This indicatesthe reducing dispersionability of the fillerathighloadingsinthezincmatrix.TheaveragediameteroftheNPparticlesisfoundtobe*25nm.The distance between the nano particles in the matrix is largeenough that they are well oriented with little interfacialinteraction.The figuresalso indicatethatthe orientationof the NPs plays a very important role in the stress–strainbehaviorofthecomposite.

Thermalpropertiesofnanoparticle

Thermal energy propagates through materials via a slow diffusion-excitation process, generating quantized elastic waves known as phonons. These phonons scatter at lattice imperfections or other inhomogeneities within the material, facilitating intermolecular energy transfer. This process is more efficient than intramolecular transfer due to fewer phonon scatterings through covalent bonds compared to van der Waals interactions. The molecular arrangement promotes thermal conductivity, with one-dimensional wave packets traveling along polymeric chains and experiencing long mean free paths. However, these wave packets may be scattered by chain ends, cross-links, or interactions with other molecules.Thermal conductivity, a measure of a material's ability to conduct heat, is influenced by various factors in composites, including: (a) intrinsic conductivities of the filler and

Industrial Engineering Journal
ISSN: 0970-2555
Volume : 53, Issue 5, May : 2024

matrix, (b) interface conductance between the filler and matrix, (c) size and shape of the filler, and (d) loading level of the fillers. Table 2 illustrates the dependence of thermal conductivity on filler loadings in silicone elastomer nanocomposites.

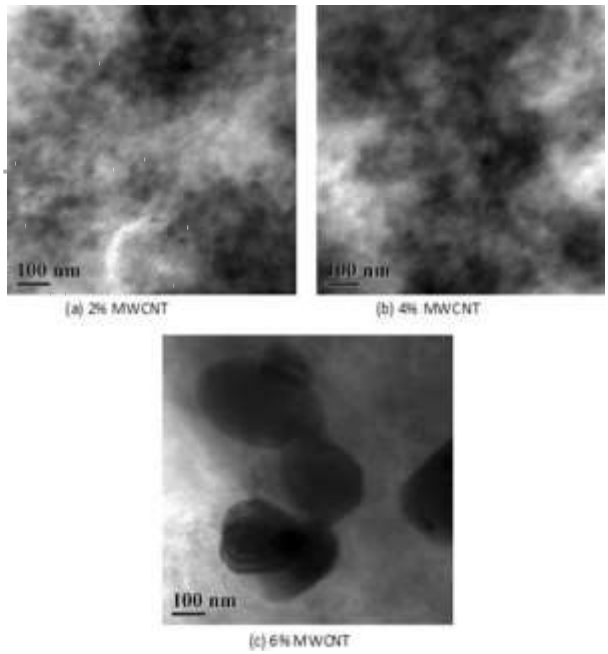

Figure 4. (a)–(c) HR-TEM image of MWCNT-filled nano particle.HR-TEM:high-resolutiontransmissionelectronmicroscopy;MWCNT:multiwalledcarbonnanotube.

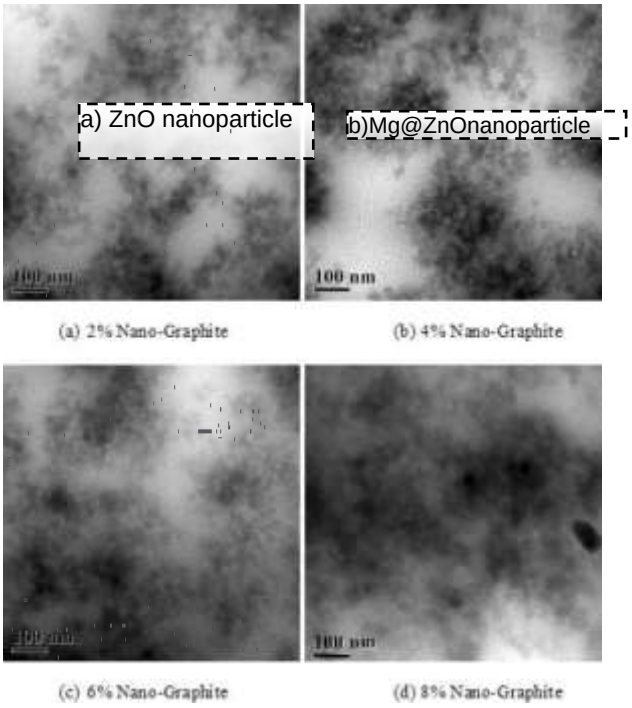

Figure 5. (a)–(d) HR-TEM image of nanoparticle. HR-TEM: high-resolutiontransmissionelectronmicroscopy.

of NG.Kumari[25]illustratedthatthethermalconductivityofMWCNT-filled nanocom positesishighe rth

Industrial Engineering Journal
ISSN: 0970-2555
Volume : 53, Issue 5, May : 2024

anthatofSWCNT-fillednanocomposite,eventhoughMWCNTs

Table2.Thermalconductivityofzinc, silver nanocompositeasafunctionoffillerloadings.

Fillerloadings(%)	0	2	4	6
ThermalconductivityofSIR-MWCNT nanocomposites (W/mK)	0.200	0.296	0.344	0.440
Thermalconductivityof SIR-NG nanocomposites(W/mK)	0.200	0.222	0.268	0.310

MWCNT:multiwalledcarbonnanotubes;NPs:nano-particle.

have low thermal conductivity; this is due to the micro-structure of the MWCNTs. Secondly, the tube–tube inter-action also affects the thermal conductivity of the zincnanocomposites.CNTshaveatendencytoagglomerate due to van der Waals forces. The phonon–phononscatteringexerts a majoreffectonthe thermalconductivity values at higher temperatures. The the rmal conduct ivit yo fthen ano part iclec omposites wasmeasuredas afunctionoftemperature (30–90°C);measurements were performed on three samples (repeatedtwiceforeachsampleateachtemperature)foreachfiller loading. The data given in this work are the average of allthe measured values, withstandard deviation notmorethan 2%. The measured thermal conductivity as a functionof temperature is plotted in Figures 6 and 7. The

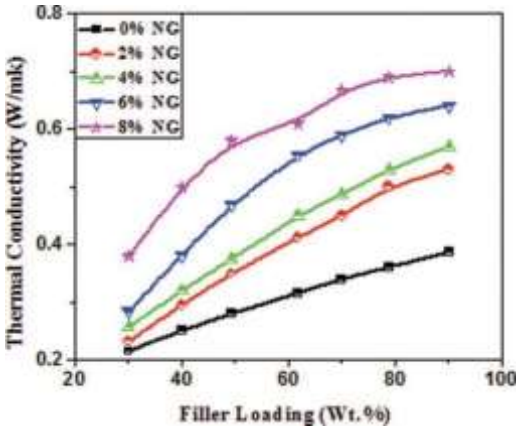

resultsshow that the thermal conductivity of SiR nanocompositesincreaseswithfillerloadingsandtemperature.Itisalso observedthat above 80°C, the polymermatrix undergoesaphasechange.Becauseofthis,theelasticityofthe matrixincreases.Therefore,above80°C,thethermalconductivityoftheSIRnanocompositesisalmost constantorincreasesnegligibly.The measured thermal conductivity is again plotted as afunctionofMWCNTandNPloadingsatdifferenttemperature in Figures 8 and 9. From the figures, it can beseenthatthethermalconductivityoftheSiRnanocompositesincreaseslinearlywithincreasingMWCNTandNPloadingsandisnearlyparallelatdifferenttemperatures,whichconfirmstheindependentin fluences of temperature and filler loading on the thermalconductivity. The percolation threshold is defined as theconcentrationbeyondwhichthe propertyofcompositematerialeitherincreasesordecreasesabruptly.FromFigures 8 and 9, it canbe

observed that above the 4%MWCNTloading,thethermalconductivityofthenanocomposites increases exponentially; this confirms thatthe percolation threshold is 4% for MWCNT-based SiRnanocomposites.Itmeansthatabove4%MWCNTloading,thefiller–fillerinter-actionsexceedpolymer–filler interactions. The agglomeration of filler particles inthenanocompositecontributestotheenhancementofthermal conductivity, because agglomerates act as regionsof heat conduction. The agglomerates decrease the contactbetween the silicone elastomer and the nanoparticles andeventuallyreducescatteringofphonons,

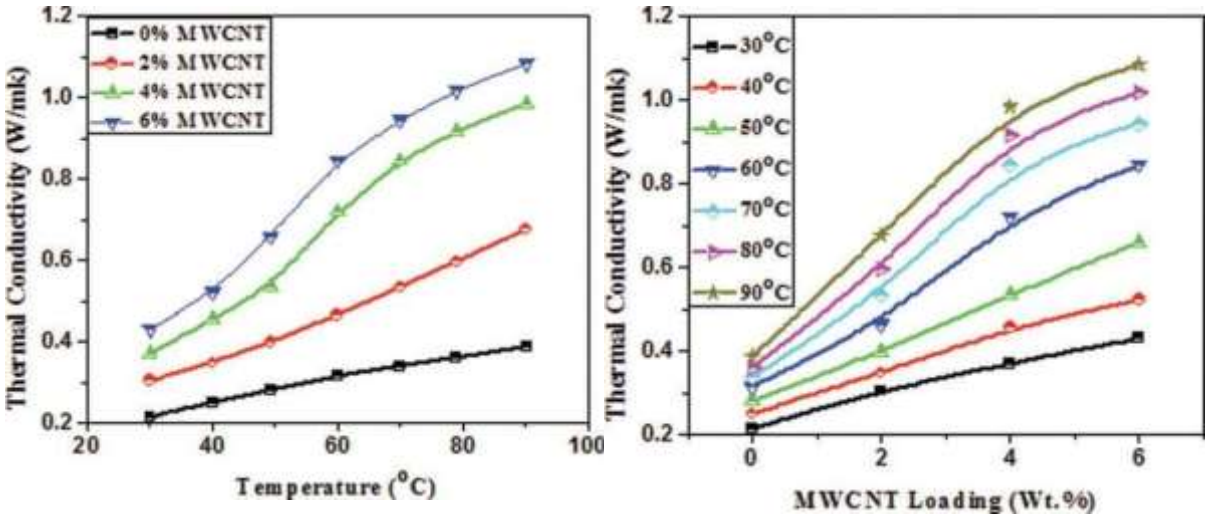

Figure 6. Variation of thermal conductivity (*k*) as a function oftemperature for MWCNT-filled nanoparticle.MWCNT:multiwalledcarbonnanotube.

Figure 7. Variation of thermal conductivity (*k*) as a function oftemperature for PLA-fillednanoparticle.

The reduced interfacial barrier between filler particles and the matrix results in decreased thermal resistance. The filler's ability to establish a conductive network within the matrix depends on its aspect ratio and loading. With increasing loading and aspect ratio, particles reach a critical percolation threshold, enabling them to make contact and form a conductive network. For example, in systems filled with NG, this percolation threshold occurs at a loading of 6%.In the rubber industry, operations generally take place within the temperature range of 100°C to 160°C. Hence, achieving high thermal conductivity at elevated temperatures is essential for various practical applications. The thermal properties (thermal conductivity, volumetric heat capacity, and thermal diffusivity) of pure polymers are significantly affected by temperature. As shown in Figures 8 and 9, the thermal conductivity of MWCNT-filled silicone rubber (SiR) nanocomposites surpasses that of NG-filled SiR at equivalent loading levels across all measured temperatures. Additionally, the inclusion of both MWCNTs and NGs substantially boosts thermal conductivity, which further rises with increasing temperatures due to the positive temperature coefficient effect and the inherently conductive nature of nanoparticles. Elastomeric thermal pads, commonly employed as thermal interface materials (TIMs), are typically thin strips used to fill gaps between heat-sensitive devices, facilitating efficient heat dissipation.

Industrial Engineering Journal
ISSN: 0970-2555
Volume : 53, Issue 5, May : 2024

Table3.Thermaldiffusivityofnanoparticle compositesasafunctionoffillerloadings.

Fillerloadings (%)	0	2	4	6
Thermaldiffusivityof SiR–MWCNT nanocomposites(mm^2/s)	0.1194	0.1906	0.2643	0.3209
Thermal diffusivity of SiR–NGnanocomposites(mm^2/s)	0.1194	0.1406	0.1800	0.2050

MWCNT:multiwalledcarbonnanotubes;NP:nano-particle.

The thermal diffusivity values of the nanoparticle composites as a function of filler loading are presented in Table 3. It is observed that the thermal diffusivity of the silicone rubber (SiR) nanocomposites increases with higher loadings of both MWCNTs and NPs. This suggests that the temperature response becomes quicker, and the SiR matrix conducts heat more efficiently with filler incorporation. Unlike thermal conductivity, no percolation behavior is observed in thermal diffusivity. However, beyond 4% loading of MWCNTs and NPs, the rate of increase in thermal diffusivity slows down.

Specifically, the thermal diffusivity of the SiR nanocomposites increases from 0.1194 mm^2/s to 0.3209 mm^2/s and 0.2050 mm^2/s for MWCNT- and NPs-filled SiR nanocomposites, respectively. Additionally, the thermal diffusivity of MWCNT-filled SiR nanocomposites is found to be 1.565 times higher than that of NPs-filled SiR nanocomposites. At a fixed filler loading (6%), MWCNT-filled silicone elastomers exhibit superior thermal performance compared to NPs-filled nanocomposites due to the higher intrinsic thermal conductivity of MWCNTs.

The temperature dependence of thermal diffusivity has been investigated for different MWCNT and NPs loadings and is depicted in Figures 10 and 11. It is observed that the thermal diffusivity of the nanocomposites decreases with increasing temperature across all filler loadings. This decrease is attributed to the higher energy phonons being thermally populated at higher temperatures, leading to stronger phonon-phonon scattering. The transport of thermal energy in non-metals is primarily governed by phonon or lattice vibrations, and phonon conduction is influenced by various types of phonon scattering processes such as phonon-phonon scattering, boundary surface scattering, and defect scattering. Minimizing these phonon scattering processes is crucial for achieving maximum thermal conductivity. Furthermore, the thermal diffusivity of the pure matrix (without filler) decreases from 0.1194 mm^2/s to 0.1070 mm^2/s.

mm^2/swhenthetemperatureisincreasedfrom30°Cto

Industrial Engineering Journal
ISSN: 0970-2555
Volume : 53, Issue 5, May : 2024

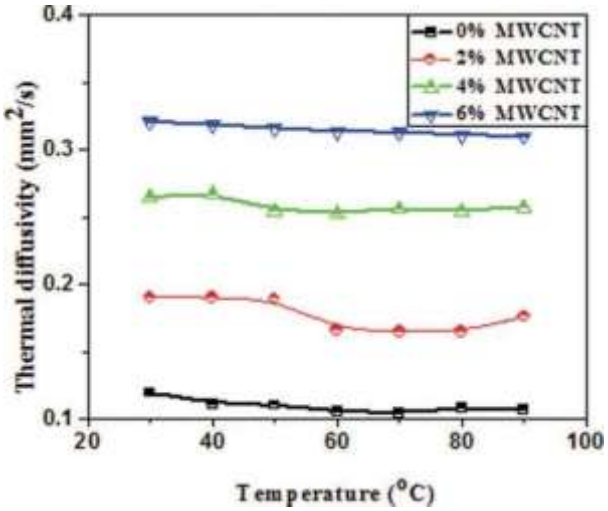

Figure 10. Thermal diffusivity (2) as a function of temperaturefor MWCNT-filled nanoparticle.MWCNT:multiwalledcarbonnanotubes.

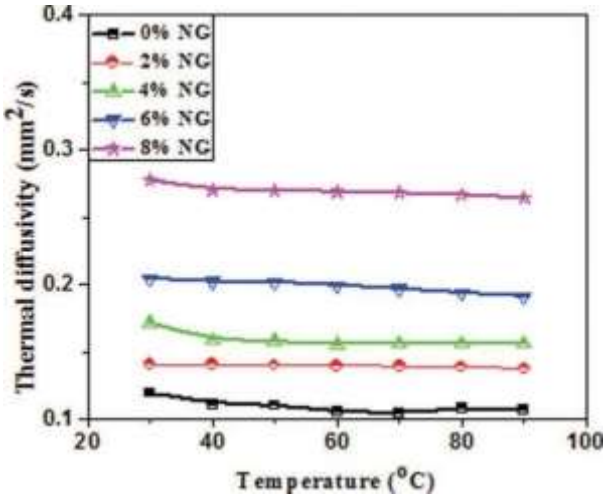

Figure 11. Thermal diffusivity (2) as a function of temperatureforPLA(poly lactic acid) - fillednanoparticle.

At 90°C, MWCNT-filled silicone rubber (SiR) nanocomposites exhibit higher thermal diffusivity compared to NPs-filled SiR nanocomposites due to the higher surface area and thermal conductivity of MWCNTs.

Regarding volumetric heat capacity, this parameter quantifies the amount of heat required to change the temperature of a material by 1°C per unit volume. It is influenced by the molecular structure and vibrational motion at the microscopic level. Table 4 presents the volumetric heat capacities of silicone elastomer nanocomposites with various MWCNT and NPs loadings.

Table4. Volumetricheatcapacityofnanoparticleasafunctionoffillerloadings.

Fillerloadings (%)	0	2	4	6
VolumetricheatcapacityofSIR–MWCNTnanocomposites(MJ/m	1.80	1.60	1.40	1.34

^{3}K)				
Volumetric heat capacity of SiR–NPs nanocomposites(MJ/m^{3}K)	1.80	1.65	1.50	1.40

MWCNT:multiwalledcarbonnanotubes;NP ; nanoparticle

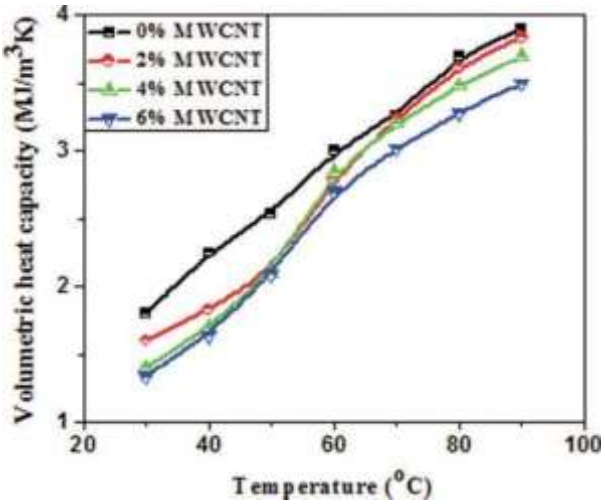

Figure 12. Dependence of volumetric heat capacity (*C*) ontemperature for MWCNT-filled nano-particle.MWCNT:multiwalledcarbonnanotubes.

The volumetric heat capacity of the silicone elastomer nanocomposites decreases from 1.80 MJ/(m³K) to 1.34 MJ/(m³K) and 1.40 MJ/(m³K) for 6% MWCNT and NPs loadings, respectively. Several factors influence the volumetric heat capacity of zinc and silver nanocomposites, including the measurement temperature, filler loading, material density, and others. However, the primary factor contributing to the enhancement in volumetric heat capacity may be the multilayered structure of MWCNTs. The weak interlayer coupling in MWCNTs can exhibit behavior ranging from 1-D to 3-D, depending on factors such as diameter and the number of walls. Furthermore, the interfaces between the boundaries of the matrix-matrix, MWCNT-matrix, or nanotube-nanotube also impact the volumetric heat capacity. Figures 12 and 13 illustrate the volumetric heat capacity of silicone elastomer with different MWCNT and NPs loadings in the temperature range of 30–90°C. It is observed that the volumetric heat capacity of all nanocomposites increases with temperature and decreases with increasing filler loading. Additionally, the volumetric heat capacity of the nanocomposites decreases faster than that of pure silicone elastomer due to the presence of thermally conductive materials within the composite.

CONCLUSIONS

Zinc-silver nanocomposites were synthesized using MWCNTs and NPs as fillers. SEM analysis revealed a uniform distribution of MWCNT and NP particles within the silver matrix. However, as the loading levels of MWCNTs and NPs increased, agglomeration occurred in the SiR matrix. HR-TEM observations further confirmed the homogenous dispersion of MWCNTs and NPs in the silicone matrix at lower loadings (2% and 4%), while agglomeration was evident at higher loadings (6% and 8%). The average diameter of MWCNTs was approximately 20 nm, whereas that of NPs was around 25 nm.

Industrial Engineering Journal
ISSN: 0970-2555
Volume : 53, Issue 5, May : 2024

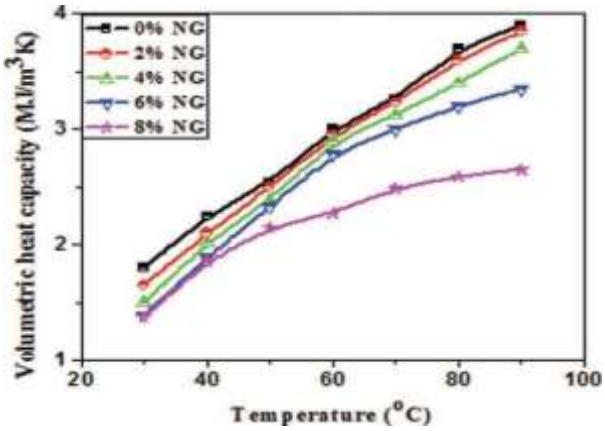

Figure 13. Dependence of volumetric heat capacity (*C*) ontemperatureforNP-fillednanoparticle.NP:nano-particle

Experimental measurements using a transient hot-wire method were conducted to determine the thermal conductivity, thermal diffusivity, and volumetric heat capacity of the zinc-silver nanocomposites at various filler fractions. The results indicated that the thermal conductivity of silicone elastomer nanocomposites increased with increasing filler loading for both MWCNT- and NP-filled systems, attributed to the conductive nature of the nanoparticles. Particularly, MWCNT-filled zinc-silver nanocomposites exhibited higher thermal conductivity compared to NPs-filled counterparts. At a constant filler loading, MWCNT-filled nanocomposites demonstrated superior thermal performance due to the higher intrinsic thermal conductivity of MWCNTs. Percolation thresholds were observed at 4% loading for MWCNT-filled systems and at 6% loading for NPs-filled systems, where thermal conductivity increased exponentially. This confirms the critical role of filler loading in enhancing thermal conductivity. filler content. he temperature coefficient effect contributes to an increase in the thermal diffusivity of zinc-silver nanocomposites with increasing MWCNT and NPs loadings, resulting in a faster temperature response due to the formation of a conductive network. Conversely, the thermal diffusivity of silicone nanocomposites decreases with rising temperature due to reduced density at higher temperatures. The volumetric heat capacity of zinc-silver nanocomposites declines with increasing filler loading, attributed to the presence of a thermally conductive material within the silver matrix. However, the volumetric heat capacity of silver zinc nanocomposites rises with increasing temperature, reflecting changes in molecular dynamics within the polymer matrix. These findings suggest that MWCNT- and NPs-filled zinc-silver nanocomposites hold promise for various applications such as elastomeric thermal pads, electronic packaging materials, heat dissipating sinks, and thermally conductive interface materials in sensitive devices, owing to their enhanced thermal properties.

Reference

1. 1.Medina,M.(2005).Servingtheunserved:informalrefusecollectioninMexico.Wastemanagement&research,23(5),390-397.
2. Gug, J., Cacciola, D., & Sobkowicz, M. J. (2015). Processing and properties of a solid energy fuelfromMunicipalSolidWaste(MSW)andrecycledplastics wastema nagemen t,35,28 3-292.
3. Al-Salem, S. M., Lettieri, P., & Baeyens, J. (2009). Recycling and recovery routes of plastic solidwaste(PSW):Areview.Wastemanagement,29(10),2625-2643.
4. Saleem, J., Ning, C., Barford, J., & McKay, G. (2015). Combating oil spill problem using plasticwastemanagement,44, 34-38.
5. Sevigné-Itoiz, E., Gasol, C. M., Rieradevall, J., & Gabarrell, X. (2015). Contribution

ofplasticwasterecoverytogreenhousegas(GHG)savingsinSpain.Wastemanagement,46,557-567.

6. Chiemchaisri,C.,Charnnok,B.,&Visvanathan,C.(2010).Recoveryofplasticwastesfromdumpsite as refuse-derived fuel and its utilization insmall gasification system.Bioresourcetechnology,101(5),1522-1527.
7. Muenmee,S.,Chiemchaisri,W.,&Chiemchaisri,C.(2015).Microbialconsortium involvingbiological methane oxidation in relation to the biodegradation ofwaste plastics in a solid wastedisposalopen dumpsite .Internatio nalBiodet erioration& Biodegrada tion,102,172-181.
8. He, Z., Li, G., Chen, J., Huang, Y., An, T., & Zhang, C. (2015). Pollution characteristics and healthrisk assessment ofvolatileor ganiccompou ndsemittedfr omdifferentplasticsolidwasterecycling workshops. Environment international, 77,85-94.
9. Dilkes-Hoffman, L.S., Pratt, S., Lant, P. A., &Laycock, B.(2019).Therole ofbiodegradableplasticinsolving plasticsolidwasteaccumulation.InPlasticstoenergy,469-505.
10. ManivongP,BourgoisE(2017)Whitepaper:Thaisugarcanesectorandsustainability.
11. PradoRDM,CaioneG,CamposCNS(2013)Filtercakeandvinasseasfertilizerscontributingtoconservationagriculture.ApplEnvironSoilSci.https://doi.org/10.1155/2013/581984
12. .PrasaraAJ,GheewalaSH(2016)Sustainabilityofsugarcanecultivation:casestudyofselecte dsitesinnorth-easternThailand.JCleanProd134:613622.https://doi.org/10.1 016/j.jclepro.2015.09.029
13. .YuttithamM,GheewalaSH,ChidthaisongA(2011)Carbonfootprintofsugarproducedfrom sugarcaneineasternThailand.JCleanProd19:21192127.https://doi.org/10.1016/j.jclepro. 2011.07.017
14. . Jenjariyakosoln S, Sajjakulnukit B, Garivait S (2013) Energy and greenhouse gas emissions reductionpotential of sugarcane field residues power generation in Thailand. Int J Environ Sci Dev 4:182– 186.https://doi.org/10.7763/IJESD.2013.V4.331
15. . Meunchang S, Panichsakpatana S, Weaver RW (2005) Co-composting of filter cake and bagasse; by-products from a sugar mill. Bioresour Technol 96:437–442.https://doi.org/10.1016/j.biortech.2004.05.02
16. Bharat,T.C.;Mondal,S.;Gupta,H.S.;Singh,P.K.;Das,A.K.Synthesisof dopedzineoxidenanoparticles:a review.MaterialsToday:Proceedings.2019,11,767-775.
17. Pillai, A.M.; Sivasankarupillai, V.S.; Rahdar, A.; Joseph, J.; Sadeghfar, F., Rajesh, K.; Kyzas, G.Z.Green synthesis and characterization of zinc oxide nanoparticles with antibacterial and antifungalactivity.JournalofMolecularStructure.2020,1211.128107.
18. Umaralikhan, L.; Jaffar, M.J.M. Green synthesis of ZnO and Mg doped ZnO nanoparticles, and itsopticalproperties.JournalofMaterialsScience: Mater ialsinE lectronics,2017.
19. Wen,Z.;Zhang,Y.;Dai,C.RemovalofPhosphatefromAqueousSolutionUsingNanoscaleZerovalentIron(nZVI).ColloidsSurf,A2014,457, 433–440.DOI:10.1016/j.colsurfa. 2014.06.0
20. TanjaNarancic,Steven Verstichel,SrinivasaReddy Chaganti,LauraMorales-Gamez,ShaneT.Kenny, Bruno De Wilde, Ramesh Babu Padamati, and Kevin E. O'Connor. Biodegradable PlasticBlends Create New Possibilities for End-of-Life Management of Plastics but They Are Not a PanaceaforPlasticPollution/2018
21. A.K. Sharma, A.K. Tiwari,A.R. Dixit, Mechanism of Nanoparticles functioning and Effects inMachiningProcesses:AReview,Mater.TodayProc.2(2015)3539–3544.
22. P.K. Singh, P. Kumar, M. Hussain, A.K. Das, G.C. Nayak, Synthesis and characterization of CuOnanoparticles using strong base electrolyte through electrochemical discharge process, Bull. Mater.Sci.39(2016)469–478.

23. P. Kumar, P.K. Singh, D. Kumar, V. Prakash, M. Hussain, A.K. Das, A novel application of micro-EDM process for the generation of nickel nanoparticles with different shapes, Mater. Manuf. Process.(2016)1–9.
24. O. Lupan, V. Cretu, V. Postica, M. Ahmadi, B.R. Cuenya, L. Chow, I. Tiginyanu, B. Viana, T.Pauporté, R. Adelung, Silver-doped zinc oxide single nanowire multifunctional nanosensor with asignificantenhancementinresponse,SensorsActuatorsBChem.223 (2016)893–903.
25. S.Kumaresan,K.Vallalperuman,S.Sathishkumar,A Novel one-step synthesis of Ag-doped ZnOnanoparticles for high performance photo-catalytic applications, J.Mater. Sci.Mate